Proceedings of the International Clay Conference, Denver, 1985, L. G. Schultz, H. van Olphen, and F. A. Mumpton, eds.,
The Clay Minerals Society, Bloomington, Indiana, 186–194 (1987).

TEXTURAL AND MINERALOGICAL RELATIONSHIPS BETWEEN FERRUGINOUS NODULES AND SURROUNDING CLAYEY MATRICES IN A LATERITE FROM CAMEROON

JEAN-PIERRE MULLER

O.R.S.T.O.M., UR 605, and Laboratoire de Minéralogie et Cristallographie, UA CNRS 09
Universités Paris 6 et 7, 2 place Jussieu, 75251 Paris Cédex 05, France

GÉRARD BOCQUIER

Laboratoire de Pédologie, Université Paris 7, 2 place Jussieu
75251 Paris Cédex 05, France

Abstract—In lateritic profiles from Cameroon, the relationships between ferruginous nodules, in which the texture has been inherited from the parent rock, and surrounding red and yellow matrices, in which the original rock texture has disappeared, were investigated by optical and scanning electron microscopy and by electron microprobe, X-ray powder diffraction, infrared, and electron spin resonance analyses. An orderly succession of changes was found for kaolinite from the ferruginous nodules to the clayey matrices as follows: (1) successive generations of the clay, each of smaller particle size; (2) concomitant decrease in degree of crystallinity; (3) increase in amount of iron substitution; and (4) decrease in the degree of orientation relative to the foliate texture of the parent gneiss. Correlative changes were also observed for associated iron oxides: (1) progressive decrease in the overall content of iron oxides; (2) decrease in the content of hematite (containing a minor amount of Al substitution); and (3) an increase in the content of Al-substituted goethite. These data suggest successive transformations from the ferruginous nodules to the surrounding clayey matrices, although progressive recrystallization may have taken place due to variation of the geochemical conditions of weathering of the original rock.

Key Words—Aluminum, Goethite, Hematite, Iron, Kaolinite, Laterite, Nodules, Texture.

INTRODUCTION

Most laterite formations of central Africa that formed in a humid climate and under forest cover show a consistent pattern of development from the bottom to the top of the profiles (Stoops, 1967; Bocquier *et al.*, 1984) as follows (Figure 1A): (1) a lower saprolite; (2) an intermediate nodular horizon composed of indurated ferruginous nodules (according to Brewer, 1964) surrounded by loose and clayey red and yellow matrices; and (3) an upper horizon mainly composed of a yellow clayey matrix. Weathering of the parent rock apparently takes place with little textural change. Millot and Bonifas (1955) and numerous other authors have shown that the weathering products commonly replicate the texture and structure of the original rock in both the saprolite and in some of the ferruginous nodules in the overlying nodular horizon. The secondary products of these materials are chiefly kaolinite and iron oxides which coexist with resistant primary minerals, such as quartz and muscovite. In contrast, the clayey matrices are characterized by the absence of original rock texture and structure. The principal mineralogical components of these matrices are also kaolinite and iron oxides (together with stable primary minerals), but these minerals have different crystal chemical characteristics (structural order, substitution rate, etc.) than those found in the saprolite and in the nodules (Herbillon, 1980; Didier *et al.*, 1983; Cantinolle *et al.*, 1984).

The present report compares the textural and crystal chemical characteristics of ferruginous nodules whose texture and structure are inherited from a parent granite gneiss with the surrounding clayey matrices.

MATERIALS AND METHODS

Materials

About 100 weathering profiles derived from gneissic granite in a tropical rain forest in central Cameroon have been described in detail by Sarazin *et al.* (1982) and Muller and Bocquier (1986). Seven of them in which the original rock structure and texture are the best preserved in the soil profiles have been selected for the present study. About thirty samples were taken from each profile.

Ferruginous nodules in these profiles are of two chief types (Figure 1): (1) Large nodules are 20–80 mm in diameter, irregular in shape, have textures more or less inherited from original gneiss that grade into the surrounding matrix. They are the more abundant type of nodule in the profiles studied. (2) Small nodules are

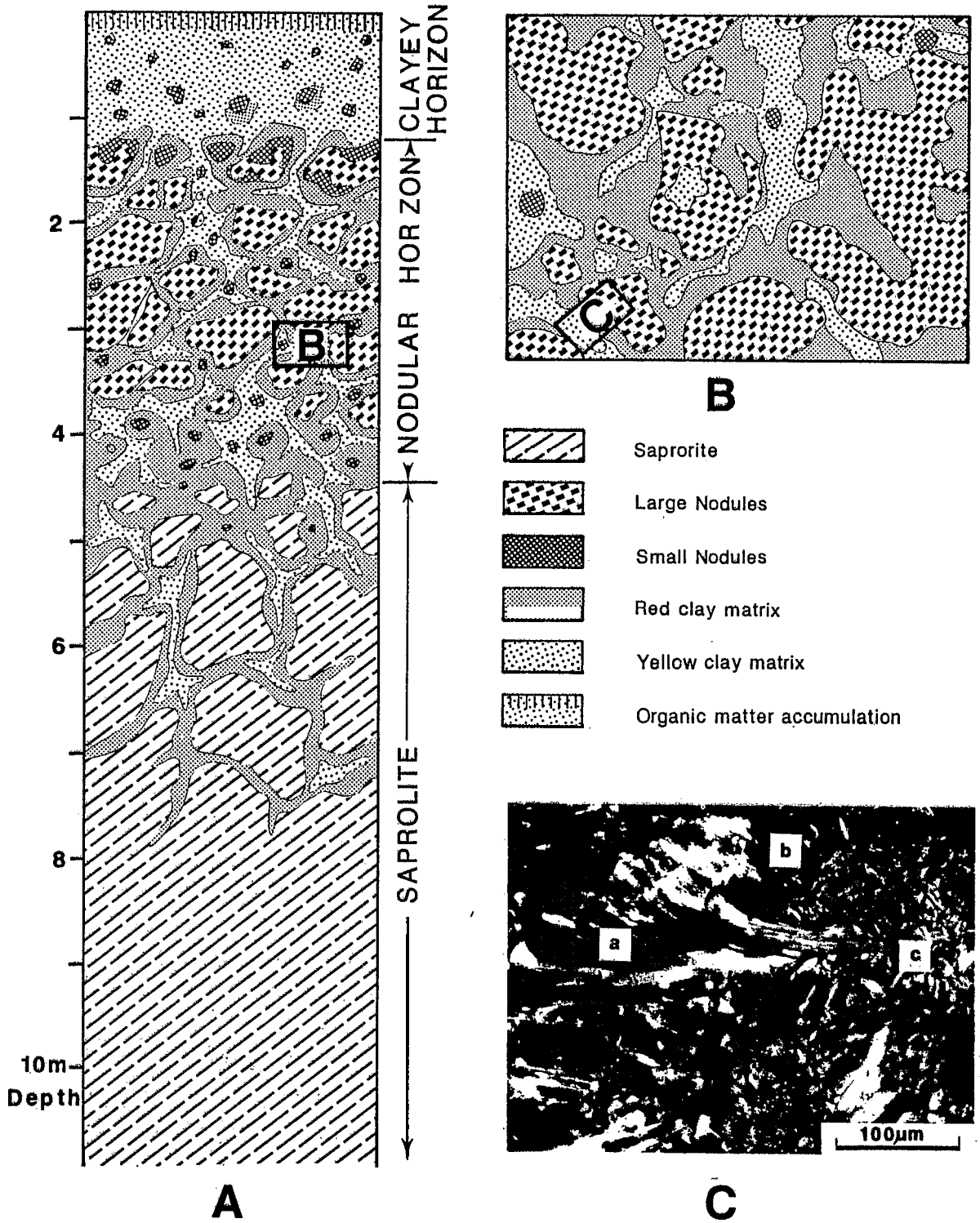

Figure 1. (A) Schematic representation of a laterite profile, Cameroon; (B) sketch of the relative distribution of matrices within an impregnated block of material from the nodular horizon; (C) optical micrograph showing the transition between a ferruginous nodule (note the inherited gneissic texture and the large crystallites of kaolinite) and clayey matrices (note the random texture and the smaller crystallites of kaolinite). a = ferruginous nodule; b = red clayey matrix; c = yellow clayey matrix.

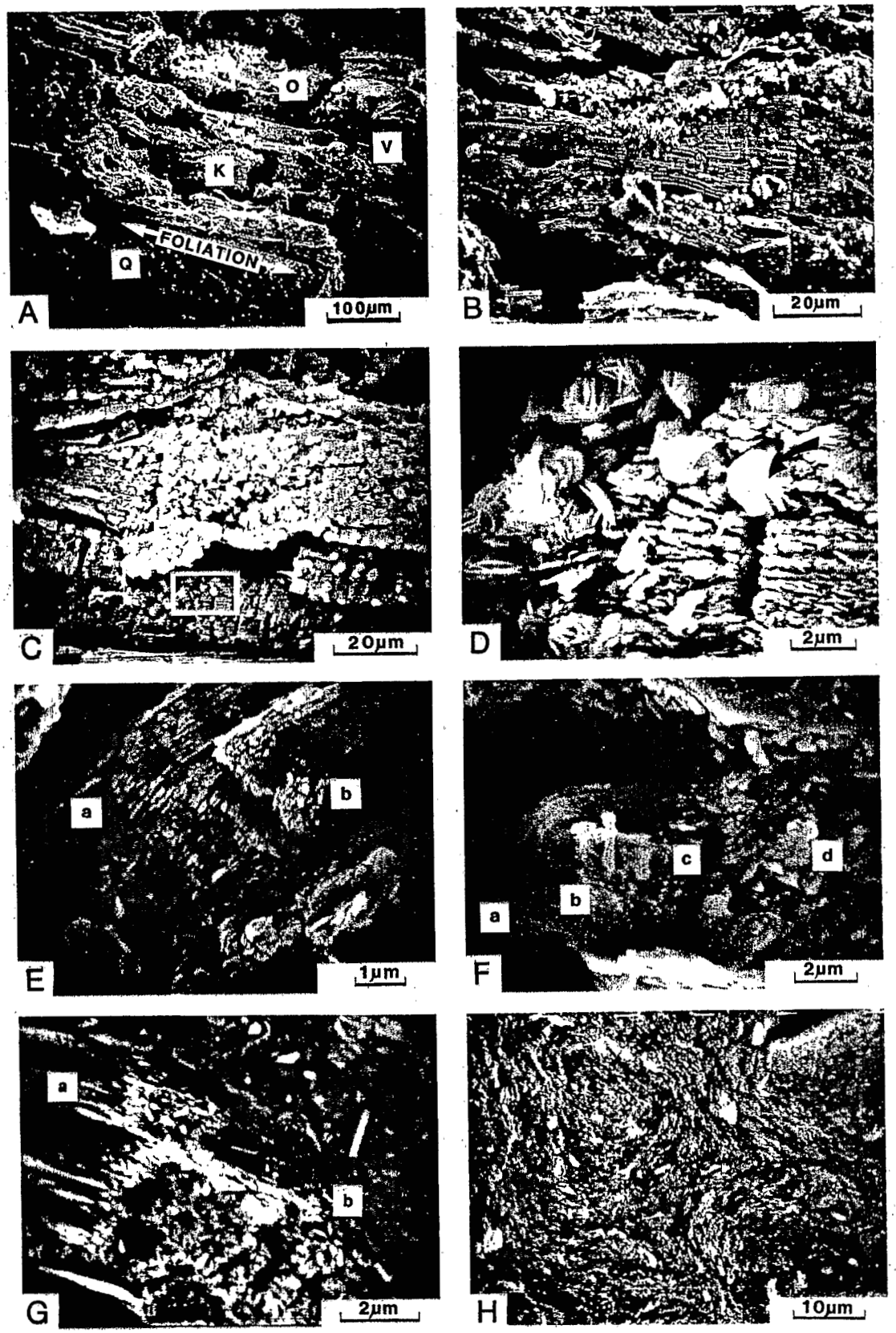
O
V
K
FOLIATION
Q
100µm
A
20µm
B
20µm
C
2µm
D
a
b
1µm
E
c
d
b
a
2µm
F
a
b
2µm
G
10µm
H

less than 20 mm in diameter, oval in shape, have sharp boundaries, and do not display the gneissic rock texture. Only the former are taken into account in this study. The smaller nodules were studied previously by Muller and Bocquier (1986).

The relationships between large nodules having inherited rock texture and surrounding clayey matrices were studied at different levels in the nodular horizon. Indeed, the nodules become more and more indurated and the original rock texture progressively less distinct upward in the horizon.

As shown schematically in Figures 1B and 1C, macroscopic and microscopic sections display an ordered relationship and gradual transition from the ferruginous nodules to a red clayey matrix and to a yellow clayey matrix. Textural, chemical, and mineralogical analyses were carried out on each of these three types of weathered materials.

Methods

Samples were impregnated with epoxy resin, and thin sections were prepared for petrographic examination. Fracture surfaces of clods were coated with gold and examined in a JEOL JSM 20 scanning electron microscope (SEM) at 20 kV. Quantitative elemental analyses were obtained on thin sections using an electron microprobe (Camebax) equipped with an EDS ORTEC multiline analyzer. Semiquantitative elemental analyses of clods were also obtained during SEM examination by energy dispersive X-ray techniques (EDX).

X-ray powder diffraction (XRD) data were obtained using CoKα radiation (40 kV, 40 mA) and a Philips PW 1730 vertical goniometer at scanning rates of 0.25 or 0.125°2θ/min. The degree of Al substitution in the goethite structure was estimated from 111 XRD line shifts using Vegard's rule. The degree of Al substitution in the hematite structure was calculated according to the quadratic equation of Perinet and Lafont (1972) after determining the unit-cell parameters by the method of William (1964).

Infrared (IR) absorption spectra were recorded in a FTIR Nicollet DX spectrograph on samples pressed in KBr. Peak intensities were calculated after an automatic baseline correction. Electron spin resonance (ESR) measurements were made at 298 K on an X-band Varian CSE 109 spectrometer, using 100 kHz modulation and 40 mW incident microwave power. Calibrated quartz tubes were filled with 50 mg of powdered samples which had been pretreated by the complexing procedure of De Endredy (1963) to remove Fe oxides.

RESULTS

Petrographic results

Ferruginous nodules. In the central part of the ferruginous nodules, especially the less indurated ones, textures of the parent gneiss were inherited at macroscopic, microscopic, and ultramicroscopic scales. For example, the SEM shown in Figure 2A illustrates the preservation of the original foliation of the gneiss, as defined by lithologic layering and the planar orientation of grain boundaries (Turner and Weiss, 1963). In Figure 2B a large crystallite of kaolinite (150 μm in diameter) appears to be pseudomorphous after mica flakes that originally were parallel to the rock cleavage, typical of *in situ* weathering as described by several authors (e.g., Bisdom *et al.*, 1982). Iron oxides occur at the boundaries between the large kaolinite booklets and interparticle voids.

Figure 2C shows another face-to-face packing of large crystallites of kaolinites. Kaolinite lamellae (40 μm in diameter) are continuous and close-packed at the edges of the aggregates, but they appear to be split into much smaller crystallites (2–5 μm in diameter) separated by cracks perpendicular to basal planes (best seen in Figure 2D) in the central part. Moreover, these smaller kaolinite crystals have been noted only where iron oxide has accumulated in the form of rosettes of intertwinned hematite platelets (see also mineralogy discussed above). Note, however, in Figure 2C that the original phyllitic texture inherited from mica is preserved.

At the periphery of the ferruginous nodules, particularly the more indurated ones, gneissic texture is macroscopically less distinct, and optically the large crystallites of kaolinite appear to be less abundant. In SEM, as in Figure 2E, even smaller kaolinite crystallites (0.5

←

Figure 2. Scanning electron micrographs of: (A) slightly indurated ferruginous nodule showing inherited gneissic texture (Q = quartz; K = pseudomorphs of kaolinite; O = iron oxides; V = voids); (B) detail of a large crystallite of kaolinite apparently pseudomorphous after mica; (C) large crystallites of kaolinite from a ferruginous nodule—low magnification micrograph showing close-packed lamellae of kaolinite at edges of aggregate; (D) detail of outlined rectangle in Figure 2C, showing smaller crystallites of kaolinite and rosettes of hematite (arrow); (E) a ferruginous nodule showing textures of different generations of kaolinite (a = preservation of original phyllitic texture by large lamellae of kaolinite, b = disruption of this texture by zones of smaller crystallites of kaolinite); (F) a ferruginous nodule showing spatial relationship between mica and successive generations of kaolinite (a = mica, b = exfoliated and large crystallite of kaolinite, c = smaller crystallites of kaolinite packed face-to-face (texture of precedent kaolinite is preserved), d = small crystallites of kaolinite in random texture); (G) the transition between (a) a ferruginous nodule and (b) the surrounding red clayey matrix showing same spatial relationship between large and small crystallites of kaolinites as in Figure 6F; (H) red clayey matrix showing "microaggregates" of small crystallites of kaolinites.

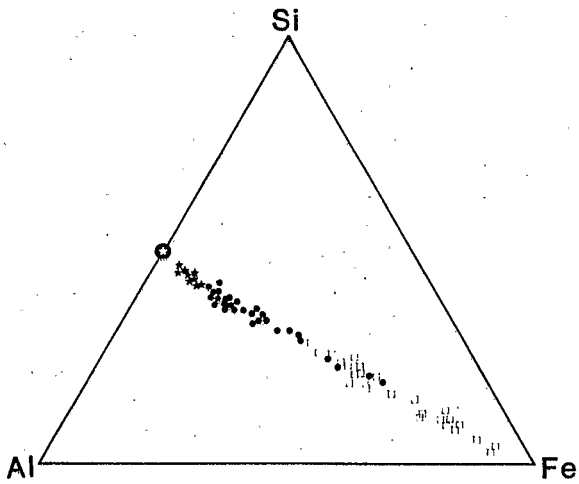

Figure 3. Chemical compositions in terms of Si, Al, and total Fe expressed as Fe^{3+}. Microprobe analyses. □ = ferruginous nodules; ● = red clayey matrix; ★ = yellow clayey matrix; ✪ = ideal kaolinite.

μm in diameter) are less oriented with respect to the larger lamellae of kaolinite (or relict mica). Figure 2F shows an orderly relationship between (a) close-packed lamellae of residual mica (identified by the presence of K in semi-quantitative analysis), (b) exfoliated large crystallites of kaolinite, (c) smaller crystallites of kaolinite, but which are still parallel to the lamellae of the exfoliated kaolinite, and (d) randomly oriented small crystallites of kaolinites. A similar sequence can be seen in Figure 2G that corresponds to the progressive macroscopic transition from ferruginous nodules to surrounding red clayey matrices shown in Figure 1C.

Clayey matrices. Both red and yellow clay matrices are characterized by a random arrangement of kaolinite crystallites, <1 μm in diameter, as has been reported elsewhere for similar materials (Eswaran, 1983). The crystal size of the kaolinites is so small in the yellow clayey matrices that these matrices appear almost optically isotropic; however, new textures are apparent, particularly in the red clayey matrices wherein kaolinite crystallites tend to be arranged concentrically (Figure 2H) in what has been called "microaggregates" (Muller, 1977; Chauvel *et al.*, 1983).

Geochemical results

In situ quantitative microprobe analyses of the secondary products in thin sections are presented in Figure 3. From these data: (1) the materials appear to be a mixture of kaolinite (Al/Si ratio is constant) and variable amounts of iron oxides; (2) the amount of iron appears to decrease from the ferruginous nodules (40–90% Fe_2O_3) to the red clayey matrix (10–50% Fe_2O_3), to the yellow clayey matrix (<12% Fe_2O_3); and (3) the iron appears to be progressively homogenized from the ferruginous nodules to the yellow clayey matrix, as is shown by a decrease in the scatter of the points in the diagram.

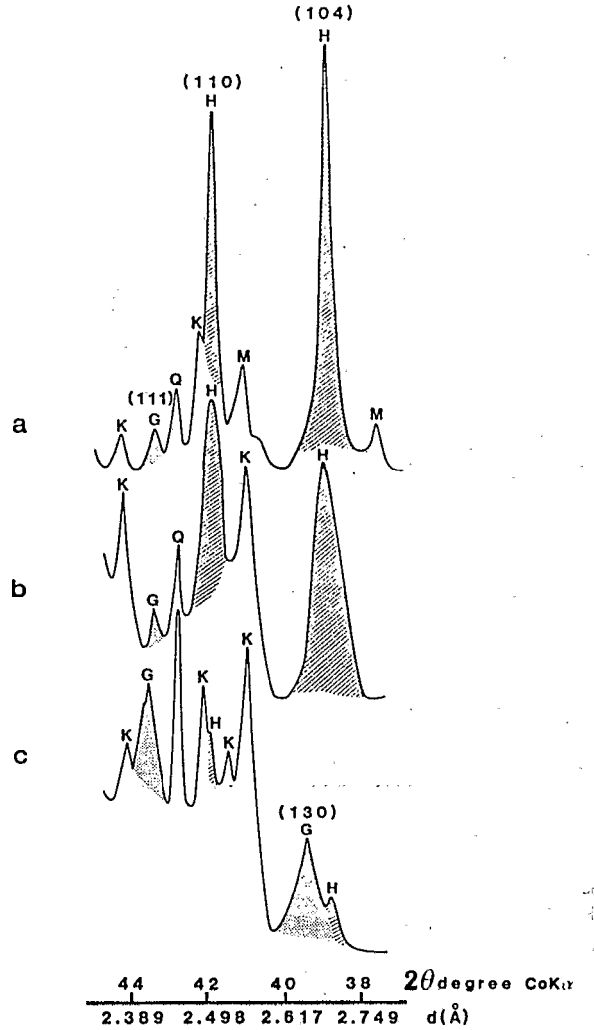

Figure 4. X-ray powder diffraction patterns of (a) ferruginous nodule; (b) red clayey matrix; (c) yellow clayey matrix. (111) = Miller indices of reflection. K = kaolinite; H = hematite; G = goethite; Q = quartz; M = muscovite-2M_1.

X-ray powder diffraction results on iron minerals

Hematite and goethite coexist in all the materials examined; however, as the iron content decreases and the color changes from red (5R) to yellow (7.5YR) (Munsell Color Chart, 1954), the iron oxide changes from almost exclusively hematite in the ferruginous nodules to predominantly goethite in the yellow clayey matrix.

Hematite. The XRD patterns of the hematite in the ferruginous nodules are different from those of hematites in the red clayey matrix (Figures 4a and 4b).

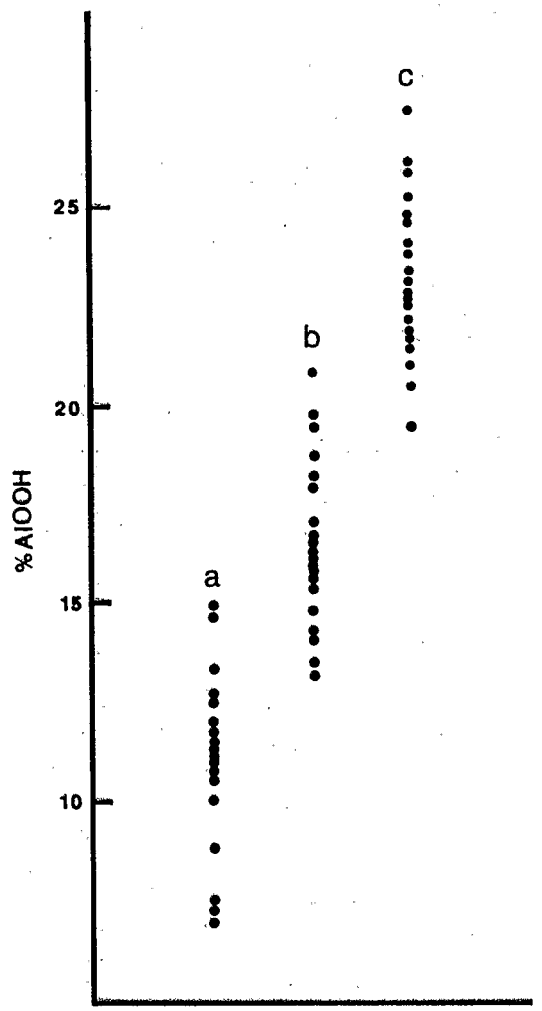

Figure 5. Plot of Al-substitution rate in goethites of (a) ferruginous nodules; (b) red clayey matrix; (c) yellow clayey matrix; expressed in % AlOOH.

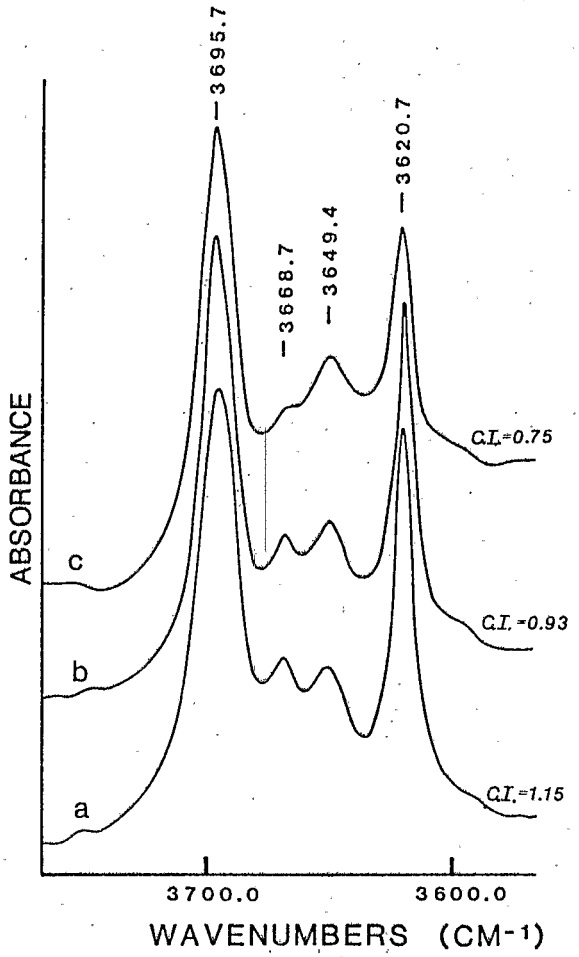

Figure 6. Infrared OH-stretching vibrations of selected kaolinites. (a) ferruginous nodules; (b) red clayey matrix; (c) yellow clayey matrix.

as follows: (1) a small shift in the 110 reflection towards lower d-values in the latter materials; (2) a broadening of the 104 and 110 reflections, attributed to a reduced growth of hematite crystals in the *Z*-direction in the presence of Al (Schwertmann *et al.*, 1979), but which can also be a result of decreased particle size and/or crystallinity; and (3) an inversion of the intensity ratios of the 104 and 110 reflections, which is probably due to a change in the amount of Al in the crystal structure (Schwertmann *et al.*, 1977). (Hematite in the yellow clayey matrices was not examined because of its low concentration and intimate occurrence with goethite and kaolinite.)

Using the XRD vs. Al-substitution data developed by Perinet and Lafont (1972), the degree of Al substitution calculated for 15 samples ranges from 3 to 6% in the ferruginous nodules and from 5 to 9% in the red clayey matrices. More quantitative analyses, however, needed to state precisely the scatter in the data points and the overlap of the different populations is in progress, using the procedure of Kampf and Schwertmann (1982) for the concentration of oxides.

Goethite. Although the differences in the properties of goethite may be related to both Al-for-Fe substitutions and structural defects (Schulze and Schwertmann, 1984), the amount of Al substitution may be estimated from the position of the 111 XRD reflection (Schulze, 1984). Data for Al content of goethite in about 20 samples of ferruginous nodules and red and yellow matrices are shown on Figure 5. The Al content of the goethite increases from the ferruginous nodules (7–15%) to the red clayey matrices (13–21%) to the yellow matrices (19–28%). These data agree with those reported by Fitzpatrick and Schwertmann (1982) who found that in lateritic environments Al substitution is much lower in red Plinthite than in yellow clayey matrices. Moreover, the comparison of the Fitzpatrick and Schwertmann (1982) data with our hematite data shows

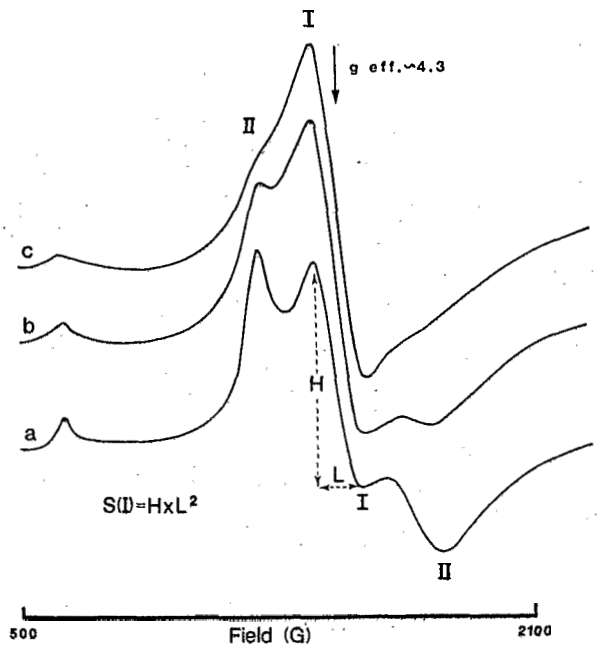

Figure 7. Electron spin resonance spectra of selected kaolinites. g_{eff} = 4-band splitting into their components I and II. (a) = ferruginous nodule; (b) = red clayey matrix; (c) = yellow clayey matrix.

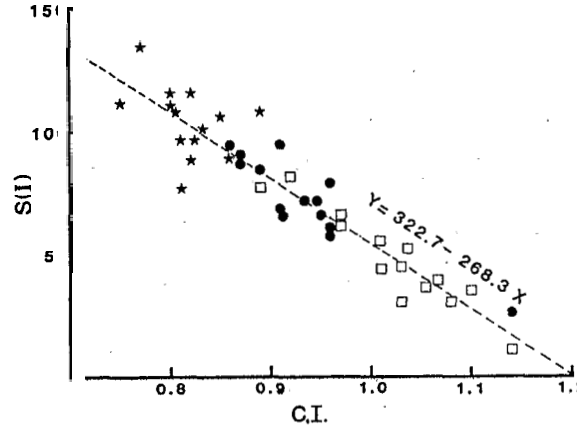

Figure 8. Correlation of infrared crystallinity index (C.I.) and S(I), the area of the internal g_{eff} = 4 signal I, expressed in arbitrary units. □ = ferruginous nodules; ● = red clayey matrix; ★ = yellow clayey matrix.

that in each type of material goethite is more Al rich than the coexisting hematite. These results agree with those reported by Nahon *et al.* (1977).

Infrared spectroscopic results for kaolinite

Most methods used to estimate the degree of order or disorder in kaolinite are based on XRD data and are somewhat limited for soil materials such as laterites, that are rich in iron oxides and quartz. IR techniques avoid such limitations (Parker, 1969). Cruz *et al.* (1982) showed that interlamellar cohesion energy increases with the degree of layer stacking disorder. Giese and Datta (1973) showed that this disorder is intimately related to the orientation of inner-surface hydroxyls. Inner-surface hydroxyls, in turn, have been found to give rise to four OH-stretching bands in IR spectra (Rouxhet *et al.*, 1977). Barrios *et al.* (1977) found a wide distribution of both absolute and relative intensities of the bands at 3669 and 3649 cm^{-1} as a function of the degree of ordering of kaolinites, giving rise to a crystallinity index, defined as C.I. = I(3669 cm^{-1})/I(3649 cm^{-1}). According to Cases *et al.* (1982), this cristallinity index corresponds well with those based on XRD data, and C.I. decreases with decreasing degree of order.

OH-stretching bands of kaolinites selected from the different materials examined in the present work are presented in Figure 6. The corresponding C.I. values range from 1.15 for ferruginous nodules to 0.75 for yellow clayey matrix. The C.I. of kaolinite from the red clayey matrix is intermediate.

Electron spin resonance of Fe-bearing kaolinite

Angel and Hall (1973) and Meads and Malden (1975) showed from ESR spectroscopy that small (<2.5%, according to Mestdagh *et al.*, 1980) and variable amounts of iron substitute in the octahedral layer of kaolinite. Such substitutions produce two components near g = 4 that are related to Fe^{3+} occupying two distinct sites in the structure of the kaolinite (centers I and II, Figure 7). The relative intensities of these two components correlate with the crystallinity of the kaolinite as follows: (1) center I is associated with layer stacking disorder; and (2) center II corresponds to domains of greater crystallinity and regular stacking (Jones *et al.*, 1974). The degree of "kaolinite perfection" and the related amount of iron substitution in I sites are closely related (Mestdagh *et al.*, 1980).

From the ESR spectra for kaolinites from the various materials examined here (Figure 7), all the kaolinites appear to be iron bearing, in agreement with Herbillon *et al.* (1976) and Mendelovici *et al.* (1979). Moreover, the relative intensity of the signal from center I with respect to center II increases from the ferruginous nodules (Figure 7a) to the yellow clayey matrices (Figure 7c), suggesting more Fe substitution in the latter. Figure 8 shows a reasonable agreement (r^2 = .87) between the integrated area (intensity × square of linewidth peak-to-peak, expressed in arbitrary units (Mestdagh *et al.*, 1980) of the signal from center I (S(I)) and the IR crystallinity index (C.I.).

DISCUSSION AND CONCLUSIONS

The gradual transition analyzed at different scales between some lateritic ferruginous nodules and their

Table 1. Comparative textural and crystal chemical characteristics of the ferruginous nodules and their surrounding clayey matrices in the nodular horizon.

Textures		Ferruginous nodules	Red clayey matrices	Yellow clayey matrices
		Inherited rock texture	Soil texture	
Iron oxides	Fe_2O_3 (%)	>40	10–50	<12
	Mineralogy	Al-hematite (3–6% Al) + Al-goethite (7–15% Al)	Al-hematite (5–9% Al) + Al-goethite (13–21% Al)	Al-goethite (19–28% Al)
Kaolinites	I.R. Crystallinity index (C.I.)[1]	0.95–1.15	0.85–0.95	0.75–0.85
	E.S.R. S(I)[2]	25–75	50–90	75–130

[1] C.I. = I(3669 cm^{-1})/I(3649 cm^{-1}).
[2] S(I) = intensity × square of linewidth peak-to-peak of "I" E.S.R. signal near g = 4.3 (arbitrary units).

surrounding loose and clayey matrices corresponds to progressive and correlative changes in textures, geochemistry, mineralogy, and crystal chemistry of both kaolinites and iron oxides (Table 1). An orderly succession of changes was found for kaolinite from ferruginous nodules to clayey matrices as follows: (1) successive generations of the clay, each of smaller particle size: (2) concomitant decrease in degree of crystallinity; (3) increase in amount of iron substitution; and (4) decrease in the degree of orientation relative to the foliate texture of the parent gneiss. In the same manner, one observes for the iron oxides: (1) progressive decrease in their overall amount; (2) decrease in the content of hematite, containing a relatively small amount of Al substitution; and (3) an increase in the content of substituted goethite, containing a relatively large amount of Al.

Because of their inherited rock texture, i.e., the size and orientation of kaolinite particles are similar to the precursor, the ferruginous nodules seem to be an earlier stage of weathering than the surrounding matrices. If this is so, successive alterations from the nodule state to the red and then presumably also to the yellow clayey matrix state suggest an *in situ* transformation of minerals in the nodules to related minerals of a different age in the matrices. We have not proven, however, that the kaolin and iron oxide minerals in the nodules have not actually dissolved and reprecipitated in slightly different form and with different chemical compositions in the matrices, in which case, the minerals could be of similar ages and formed in response to different geochemical conditions that, with time, migrated generally inward toward centers of the nodules and downward in the soil profile.

ACKNOWLEDGMENTS

We are grateful to G. Calas for laboratory facilities, to MM. Locati and Morin for their technical assistance and to G. Calas, U. Schwertmann, and R. Fitzpatrick for helpful discussions.

REFERENCES

Angel, B. R. and Hall, P. L. (1973) Electron spin resonance studies of kaolinite: in *Proc. Int. Clay Conf., Madrid, 1972*, J. M. Serratosa, ed., Div. Ciencias C.S.I.C., Madrid, 47–60.

Barrios, J., Plançon, A., Cruz, M. J., and Tchoubar, C. (1977) Qualitative and quantitative study of stacking faults in a hydrazine treated kaolinite. Relationships with the infrared spectra: *Clays & Clay Minerals* **25**, 422–429.

Bisdom, E. B. A., Stoops, G., Delvigne, J., Curmi, P., and Altemuller, H. J. (1982) Micromorphology of weathering biotite and its secondary products: *Pedologie* **32**, 225–252.

Bocquier, G., Muller, J. P., and Boulangé, B. (1984) Les latérites. Connaissances et perspectives actuelles sur les mécanismes de leur différenciation: *Livre Jubilaire Cinquantenaire A.F.E.S.*, Paris, 123–138.

Brewer, R. (1964) *Fabric and Mineral Analysis of Soils:* Wiley, New York, 470 pp.

Cantinolle, P., Didier, P., Meunier, J. D., Parron, C., Guendon, J. L., Bocquier, G., and Nahon, D. (1984) Kaolinites ferrifères et oxyhydroxydes de fer et d'alumine dans les bauxites des Canonettes (S.E. de la France): *Clay Miner.* **19**, 125–135.

Cases, J. M., Lietard, O., Yvon, J., and Delon, J. F. (1982) Etude des propriétés cristallochimiques, morphologiques, superficielles de kaolinites désordonnés: *Bull. Minéralogie* **105**, 439–455.

Chauvel, A., Soubiès, F., and Melfi, A. (1983) Ferrallitic soils from Brazil. Formation and evolution of structure: *Sciences Geol.* **72**, 37–46.

Cruz, M., Sow, C., and Fripiat, J. J. (1982) Etude par spectrométrie infrarouge des kaolinites désordonnées: *Bull. Minéralogie* **105**, 493–498.

De Endredy, A. S. (1963) Estimation of free iron oxides in soils and clays by a photolytic method: *Clay Miner.* **5**, 209–217.

Didier, P., Nahon, D., Fritz, B., and Tardy, Y. (1983) Activity of water as a geochemical controlling factor in ferricretes. A thermodynamic model in the system kaolinite Fe-Al oxihydroxides: *Sciences Geol.* **71**, 35–44.

Eswaran, H. (1983) Characterization of domains with the scanning electron microscope: *Pedologie* **38**, 41–54.

Fitzpatrick, R. W. and Schwertmann, U. (1982) Al-substituted goethite. An indicator of pedogenic and other weathering environments in South Africa: *Geoderma* **27**, 335–347.

Giese, R. F. and Datta, P. (1973) Hydroxyl orientation in kaolinite, dickite, and nacrite: *Amer. Min.* **58**, 471–479.

Herbillon, A. J. (1980) Mineralogy of oxisols and oxic materials: in *Soils With Variable Charge*, B. K. B. Theng, ed., N.Z. Soc. Soil Sci., Wellington, 109–126.

Herbillon, A. J., Mestdagh, M. M., Vielvoye, L., and Derouane, E. G. (1976) Iron in kaolinite with special reference to kaolinite from tropical soils: *Clay Miner.* **11,** 201–220.

Jones, J. P. D., Angel, B. R., and Hall, P. L. (1974) Electron spin resonance studies of doped synthetic kaolinites. II: *Clay Miner.* **10,** 257–269.

Kampf, N. and Schwertmann, U. (1982) The 5-M NaOH concentration treatment for iron oxides in soils: *Clays & Clay Minerals* **30,** 401–408.

Meads, R. E. and Malden, P. J. (1975) Electron spin resonance in natural kaolinites containing Fe^{3+} and other transition metal ions: *Clay Miner.* **10,** 313–345.

Mendelovici, E., Yariv, S. H., and Villalba, B. (1979) Iron bearing kaolinite in Venezuelan laterites. Infrared spectroscopy and chemical dissolution evidence: *Clay Miner.* **14,** 323–331.

Mestdagh, M. M., Vielvoye, L., and Herbillon, A. J. (1980) Iron in kaolinite. The relationship between kaolinite crystallinity and iron content: *Clay Miner.* **15,** 1–14.

Millot, G. and Bonifas, M. (1955) Transformations isovolumétriques dans les phénomènes de latérisation et de bauxitisation: *Bull. Service Carte Géologique Alsace Lorraine* **8,** 3–20.

Muller, J. P. (1977) Microstructuration des structichrons rouges ferrallitiques, à l'amont des modelés convexes, Centre-Cameroun: *Cahiers ORSTOM Pédologie* **15,** 25–44.

Muller, J. P. and Bocquier, G. (1986) Dissolution of kaolinites and accumulation of iron oxides in lateritic-ferruginous nodules: mineralogical and microstructural transformations: *Geoderma* **37,** 113–136.

Munsell Color Chart (1954) *Munsell Soil Color Charts:* Munsell Color Company, Baltimore, Maryland.

Nahon, D., Janot, C., Karpoff, A. M., Paquet, H., and Tardy, Y. (1977) Mineralogy, petrography and structures of iron crusts (ferricretes) developed on sandstones in the western part of Senegal: *Geoderma* **19,** 263–278.

Parker, T. W. (1969) A classification of kaolinites by infrared spectroscopy: *Clay Miner.* **8,** 135–141.

Perinet, G. and Lafont, R. (1972) Sur les paramètres cristallographiques des hématites alumineuses: *C.R. Acad. Sci. Paris* **275,** 1021–1024.

Rouxhet, P. G., Samudacheata, N., Jacobs, H., and Anton, O. (1977) Attribution of the OH stretching bands of kaolinite: *Clay Miner.* **12,** 171–179.

Sarazin, G., Ildefonse, Ph., and Muller, J. P. (1982) Contrôle de la solubilité du fer et de l'aluminium en milieu ferrallitique: *Geochim. Cosmochim. Acta* **46,** 1267–1279.

Schulze, D. G. (1984) The influence of aluminum on iron oxides. VIII. Unit-cell dimensions of Al-substituted goethites and estimation of Al from them: *Clays & Clay Minerals* **32,** 36–44.

Schulze, D. G. and Schwertmann, U. (1984) The influence of aluminium on iron oxides. X. Properties of Al-substituted goethites: *Clay Miner.* **19,** 521–539.

Schwertmann, U., Fitzpatrick, R. W., and Le Roux, J. (1977) Al substitution and differential disorder in soil hematites: *Clays & Clay Minerals* **25,** 373–374.

Schwertmann, U., Fitzpatrick, R. W., Taylor, R. M., and Lewis, D. G. (1979) The influence of aluminum on iron oxides. II. Preparation and properties of Al-substituted hematites: *Clays & Clay Minerals* **27,** 105–112.

Stoops, G. (1967) Le profil d'altération du Bas Congo (Kinshasa): *Pédologie* **17,** 60–105.

Turner, F. J. and Weiss, L. E. (1963) *Structural Analysis of Metamorphic Tectonites:* McGraw-Hill, New York, 525 pp.

William D. E. (1964) LCR2 Fortran lattice constant refinement program: U.S. Atom. Energy Comm. Report, **IS-1052.**